Developmental Cell
Article

A Molecular Base for Cell Sorting at Embryonic Boundaries: Contact Inhibition of Cadherin Adhesion by Ephrin/Eph-Dependent Contractility

François Fagotto,[1,2,*] Nazanin Rohani,[1,2] Anne-Sophie Touret,[1] and Rui Li[1]
[1]Department of Biology, McGill University, Montreal, QC H3A 1B1, Canada
[2]These authors contributed equally to this work
*Correspondence: francois.fagotto@mcgill.ca
http://dx.doi.org/10.1016/j.devcel.2013.09.004

SUMMARY

The mechanism responsible for subdividing the embryo into individual tissues is a fundamental, yet still poorly understood, question in developmental biology. Various general hypotheses have been proposed, involving differences in cell adhesion, contractility, or contact-mediated repulsion. However, the key parameter in tissue separation, i.e., the regulation of cadherin-based adhesion at the boundary, has not yet been investigated. We show that cadherin clustering is specifically inhibited at the vertebrate notochord-presomitic mesoderm boundary, preventing formation of adhesive bonds between cells of the two different types. This local regulation depends on differentially expressed ephrins and Eph receptors, which increase cell contractility and generate a membrane blebbing-like behavior along the boundary. Inhibiting myosin activity is sufficient to induce cadherin clustering and formation of stable contacts across the boundary, causing notochord and presomitic tissues to fuse. Local inhibition of cadherin adhesion explains how sharp separation can be achieved in response to cell-cell contact signals.

INTRODUCTION

Development proceeds by successive subdivisions of the embryo into various regions/compartments and eventually into tissues and organs. Each region becomes physically delimited by a boundary that prevents further cell mixing with the adjacent cell populations. In vertebrates, most boundaries will eventually evolve into strong permanent barriers made of secreted extracellular matrix. In the early stages of separation, however, tissue boundaries are highly permeable, because cells or even whole groups of cells can freely cross them under various experimental conditions (Maghzal et al., 2010; Medina et al., 2004; Reintsch et al., 2005; Rohani et al., 2011; Wacker et al., 2000). Different schools of thought have tried to explain the nature of these boundaries: differential expression of homophilic adhesion molecules (Takeichi, 1995), quantitative differences in adhesive strength (Foty and Steinberg, 2005; Manning et al., 2010; Steinberg and McNutt, 1999; Steinberg, 1970) or in cortical tension (Harris, 1976; Krieg et al., 2008; Maître et al., 2012), or ephrin/Eph-mediated cell repulsion (Cooke et al., 2005; Durbin et al., 1998; Kemp et al., 2009). The first mechanism is unlikely to act in the early embryonic stages, where adhesion generally relies on one single cadherin (Heasman et al., 1994a, 1994b; Tepass, 1999). As for the models based on quantitative differences in adhesion or tension, they both predict that the type and strength of interactions occurring at the tissue interface should represent an intermediate value between the properties of each tissue taken separately (Krieg et al., 2008; Maître et al., 2012; Manning et al., 2010). Yet, when boundary interfaces are observed in more detail, they reveal unique characteristics that are not observed within the tissues: for instance, in *Drosophila*, prominent actomyosin cables run along the parasegmental boundaries and appear to be required to maintain separation of these compartments (Monier et al., 2010). In *Xenopus*, the ectoderm-mesoderm boundary is characterized by local cycles of attachments-detachments (Rohani et al., 2011). Whether these two examples may be related to some common principle or reflect different modes of tissue separation remains unknown, but both clearly indicate that what happens at the contact between two cell types cannot necessarily be predicted by the properties of the individual cell populations.

We have thus set out to study early tissue interfaces directly, using two models in *Xenopus*: the boundary between ectoderm-mesoderm (Rohani et al., 2011) and the subsequent partition of dorsal mesoderm into notochord and the presomitic—also called paraxial-mesoderm (Reintsch et al., 2005). Using independent approaches, both studies demonstrate that cells can sense the identity of the neighboring cells: they discriminate between "homotypic contacts" with cells of the same tissue and "heterotypic contacts" with cells of another tissue. Stable adhesion is only formed at the formers. In the case of ectoderm-mesoderm separation, we have identified ephrins and Eph receptors as the "heterotypic contact cues" and have shown that they generate Rho/Rac-dependent cycles of attachments-detachments (Rohani et al., 2011; N.R., R. Winklbauer, and F.F., unpublished data).

The effector mechanisms that mediate the actual physical separation of the two tissues have remained undetermined. What is the status of cadherins at heterotypic contacts, and how are they regulated? The study of the notochord boundary seemed particularly promising to elucidate this question: whereas cohesion

increases in both notochord and presomitic mesoderm tissues as they enter the phase of convergence-extension (Moore et al., 1995), adhesion between them seems to drop instantaneously as the boundary appears. To understand this phenomenon, we have directly investigated the status of cadherins within the tissues and at the boundary. Cadherins are known to form large multimeric clusters, which, similarly to focal contacts for integrins, are considered to be required to produce substantial adhesive force. These clusters are further connected to the actin cytoskeleton through not yet fully elucidated protein complexes that include catenins as core components (Ratheesh and Yap, 2012). In early embryonic cells, these cadherin clusters distribute along the membranes as discrete spots, called "puncta" or "spot junctions" (Tepass and Hartenstein, 1994; Winklbauer, 2009), that can be used to monitor sites of cell-cell adhesion (Cavey et al., 2008). Here, we show that loss of adhesion at the notochord boundary is not due to the exclusion of cadherins from this interface but rather to local actomyosin contractility that inhibits cadherin clustering. We further demonstrate that increased actomyosin contractility and inhibition of cadherin clustering along the boundary are a consequence of ephrin-Eph signaling, supporting a general role of these repulsive cues in vertebrate tissue separation.

RESULTS

Cadherin Clustering Is Inhibited at the Boundary Interface

The notochord boundary is already well established in late gastrula embryos (stage 12.5). It will later be "sealed" by extracellular matrix, but it is still completely "permeable," as demonstrated by the ability of single cells to rapidly sort from one tissue to the other (Reintsch et al., 2005). Macroscopically, the newly formed notochord shows little to no adhesion to the adjacent somatic mesoderm, because these two tissues freely separate from each other during microdissection. We asked whether this property corresponded to differences in adhesive structures by examining the distribution of C-cadherin, which is the only cadherin expressed at significant levels at this stage. Both endogenous cadherin and exogenously expressed C-cadherin-GFP showed essentially the same general pattern (Figures 1B and 1C). At homotypic contacts within each tissue, C-cadherin was concentrated in numerous dense spots, decorating the plasma membranes (arrows), which typically correspond to discrete adhesive contacts, also called cadherin "puncta" (Adams et al., 1998; Cavey et al., 2008; Tepass and Hartenstein, 1994; Vasioukhin et al., 2000) (Figures 1B and 1C). The boundary interface appeared, however, quite different: fewer puncta were observed (Figures 1B and 1C), and a prominent diffuse signal gave the boundary interface the appearance of a "curtain" (arrowheads). Note that groups of puncta were often found along the boundary at corners between two notochord or between two presomitic cells (Figures 1C and 1D′, yellow arrows). These structures could be well resolved by live confocal microscopy, which unambiguously demonstrated that they did not involve heterotypic contacts across the boundary but represented lateral homotypic "junctions" (Figures 1D and 1D′, yellow arrows). Quantification of C-cadherin-GFP in live explants showed that the puncta density was ten times lower at the boundary (Figures 1B′, B″, C′, and Figure S1C available online). The proportion of cadherin included in the clusters was also much smaller (Figure 1B‴). The difference was smaller in fixed samples, which can be explained by the fact that the identity of many contacts could not be established with certainty, because of imperfect membrane preservation and lower resolution, which led us to conservatively overestimate heterotypic puncta (see legends) (Figure 1C′). The average signal intensity for endogenous cadherin was also higher at the boundary (Figure 1C′), probably because of better epitope accessibility compared to homotypic clusters in fixed samples. These potential caveats made us favor live explants, and we used the former for most of our study. C-cadherin-GFP-expressing embryos developed normally despite the known sensitivity of early development (Lee and Gumbiner, 1995), indicating that this construct did not significantly alter adhesive and migratory properties under our experimental conditions. The "smooth undulating curtain" could be considered a hallmark of the boundary, sufficient on its own to unambiguously identify this structure. Although we cannot exclude the existence of other smaller scale organization/clustering outside of these puncta, our results were strongly indicative of a much more diffuse cadherin distribution at the boundary interface.

The most obvious reasons for the deficiency of cadherin clusters could be readily discarded: (1) it could not be explained by the total cadherin levels, which were only marginally lower at the boundary of live explants (Figure 1B‴); (2) cells were constantly in close apposition, as the two membranes could not be resolved (Figure 1F) and cells appeared to press against each other across the boundary (Figures 2A; Movie S1); (3) mesoderm cells did not show signs of apical-basolateral polarity at this stage (Figures S1F and S1F′); and (4) the distribution of the basic components of the adhesion complexes, β-catenin, α-catenin, and p120catenin, appeared identical to cadherin (Figures 1D, 1E, and S1G). The intensity ratio between α-catenin and cadherin signals was similar at homotypic contacts in the tissues and at heterotypic nonadhesive contacts along the boundary (Figures 1D″ and S1G‴), indicating that puncta and smooth membranes have a similar composition in terms of the core of the cadherin-associated complex. In conclusion, the scarcity of cadherin clusters at the boundary did not appear to be due to a physical gap that would prevent cadherin interactions or to an exclusion of cadherins from this interface. Rather this scarcity appeared to be related to a specific "instructive" mechanism that inhibited cadherin clustering across the boundary. This mechanism did not seem to involve disruption of the basic cadherin-catenin complex.

Inhibition of Clustering Is Independent of Cadherin Levels and Subtype

The smooth distribution of C-cadherin at the boundary appeared to be an extremely robust trait. Quantitative comparison of cadherin-GFP distribution between weakly and strongly expressing cells demonstrated that although puncta density tended to increase with cadherin levels, both at homotypic and heterotypic contacts, heterophilic contacts showed in all cases the same strong deficit in puncta density (Figures S1A–S1C). The rule applied to all of our images: compared to homotypic contacts with similar cadherin levels, heterotypic contacts always

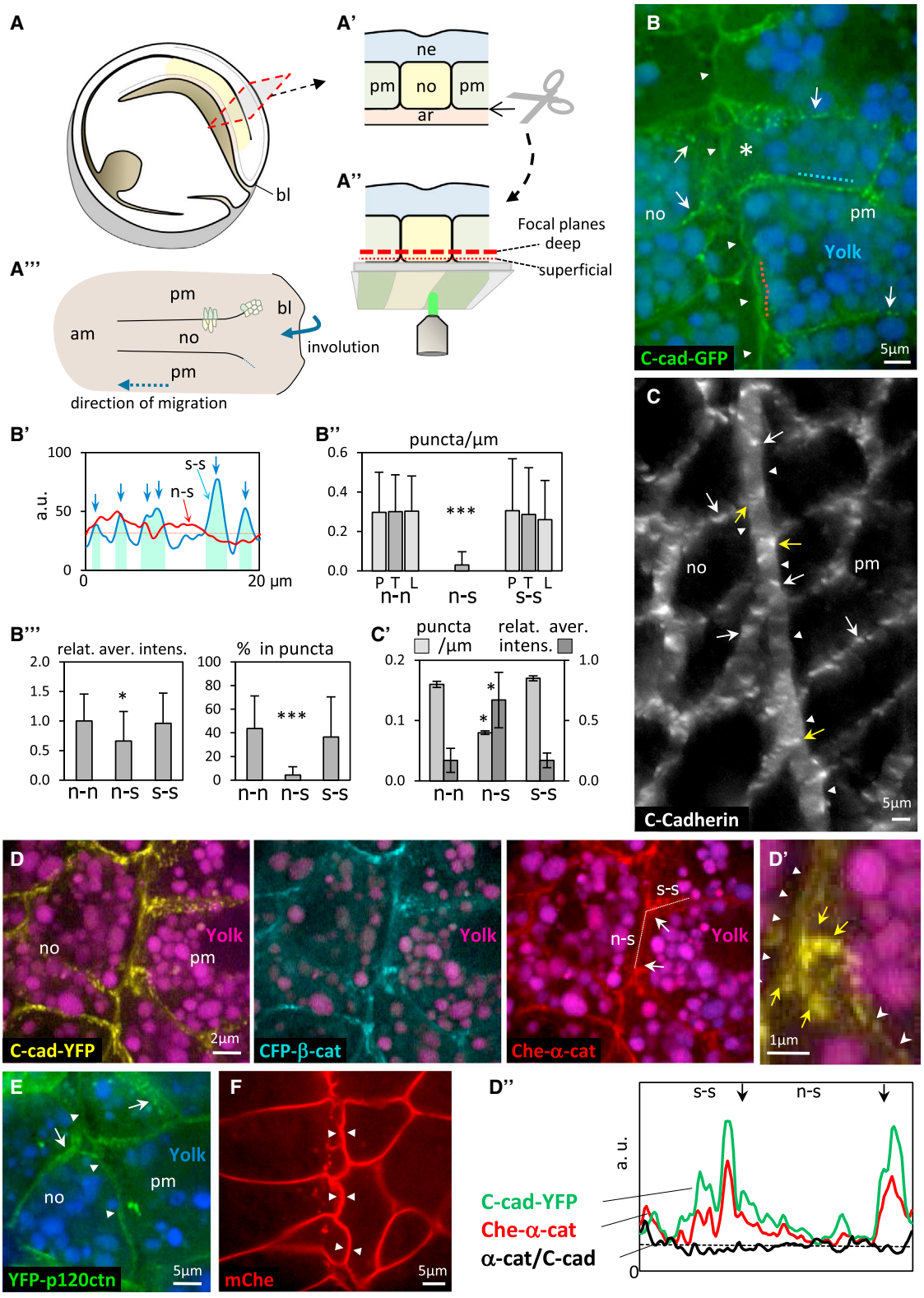

Figure 1. Inhibition of Cadherin Clustering at the Notochord Boundary

(A–A‴) Experimental setting: (A) Diagram of a late gastrula embryo. (A′) Transversal section of dorsal structures. (A″) Live confocal microscopy of dorsal explants after removal of the archenteron roof. (A‴) Ventral view of explant, with examples of cells in the region in which the boundary forms and along the mature boundary. am, anterior mesoderm; ar, archenteron roof; bl, blastopore lip; ne, neuroderm; no, notochord; pm, paraxial/presomitic mesoderm.

(legend continued on next page)

displayed a much lower number of puncta. The robustness of the process is further illustrated by the extreme example shown in Figure S1D: expression of a dominant-negative mutant of cadherin lacking the extracellular domain (ΔEcad) induces a dramatic destabilization of endogenous cadherins (Reintsch et al., 2005). We found that these cells were still able to distinguish between the different contacts, recruiting most of the remaining cadherins to form homotypic puncta (Figure S1D, yellow arrows). Taken together, our data show that the smooth pattern observed at the boundary was independent of cadherin levels, implying that clustering was locally inhibited by a specific mechanism.

The lack of clusters along the boundary was not a phenomenon specific to C-cadherin: expression of E-cadherin normally starts only at the end of gastrulation in the nonneural ectoderm (data not shown). When ectopically expressed in the dorsal mesoderm, its distribution closely followed the normal C-cadherin pattern (Figures S1E and S1E′): it formed dense spots at contacts within the tissues (arrows), while segments of smooth membrane were visible along the boundary (arrowheads). Note that two nonclassical cadherins, PAPC and AxPC, are expressed complementarily in the trunk mesoderm during gastrulation, in the paraxial mesoderm and in the notochord, respectively. However, protocadherins do not appear to function as adhesion molecules but rather as regulators of C-cadherin adhesion (Chen and Gumbiner, 2006), and ectopic PAPC expression in notochord cells was not sufficient to sort them to the presomitic mesoderm (data not shown). We conclude that cluster formation at homotypic contacts is largely independent of cadherin levels or cadherin type and that inhibition of clustering along the boundary appears to be dictated by a different and strongly dominant mechanism.

Dynamics of Boundary Behavior

In contrast to the stability of the homotypic contacts within each of the two tissues, the boundary appeared to be a remarkably dynamic region (Figures 2A and S2A). We identified two types of behavior at the boundary: a rapid undulation, resembling the flapping of a flag (Figure 2A″; Movie S1) and an equally rapid formation of transient protrusions or digitations that emanated from both tissues and intermingled (Figure 2A'; Movie S1). This behavior was quite reminiscent of classical blebbing. Time-lapse images of mosaic embryos containing single cells expressing membrane-targeted Cherry fluorescent protein (Figures S2A and S2A′) showed protrusions freely exploring the boundary interface. Cells remained almost permanently in intimate contact: as one cell would retract, the abutting cell would instantaneously fill the gap (Figure 2A). The membrane behavior could switch between undulations and emission of protrusions (Movie S1), and we hypothesized that these were manifestations of a single underlying mechanism (see below).

Induction of a "Smooth Boundary" at Ectopic Heterotypic Contacts

Expression of a LEF-VP16 fusion construct, which constitutively activates β-catenin/TCF signaling, dominantly confers somitic fate, even to cells located in the notochord (Reintsch et al., 2005). This allowed us to study single presomitic cells surrounded by notochord cells. These cells move randomly within the notochord until they contact the paraxial mesoderm, in which case they rapidly cross the boundary and irreversibly integrate into the paraxial mesoderm (Reintsch et al., 2005). To investigate the behavior of these cells at high resolution, we injected a DNA plasmid coding for both nuclear LEF-VP16 and membrane-targeted Cherry fluorescence protein (see the Experimental Procedures). At stage 12.5, most LEF-VP16-expressing cells had already sorted to the presomitic mesoderm (Reintsch et al., 2005). We confirmed that they were well integrated in the tissue, establishing numerous cadherin puncta with their neighbors (Figure S2B, arrows), and that control cells expressing membrane-Cherry alone had a normal cadherin distribution in the tissues and at the boundary (Figure S2C). We searched for LEF-VP16-expressing cells still located in the notochord and found that their contacts with the surrounding notochord cells mimicked the properties of the endogenous boundary, displaying a smooth cadherin pattern (Figure 2B, white arrowheads) and undulations (Figure 2B, yellow arrowhead) or blebbing (Figure 2A; Movie S2). These mislocalized cells were fully able to distinguish between homotypic and heterotypic contacts: we

(B) C-cadherin-GFP distribution in live explants. Vertical projection of a stack of five z planes (1 μm apart). The boundary is characterized by a smooth undulating C-cadherin-GFP signal (arrowheads) that contrasts with the punctated membranes within each tissue (arrows). Far red autofluorescence of the yolk was recolored in blue. Note the yolk-free cytoplasm along the boundary (asterisk). (B′–B″) Quantification: (B′) Line scans from membranes marked by dotted lines in (B). Blue line: Homotypic contact between presomitic mesoderm cells (s-s). Puncta appear as sharp peaks (vertical arrows). Red line: Smoother notochord-presomitic mesoderm interface (n-s). (B″) Puncta density along notochord (n-n), presomitic mesoderm (s-s), and boundary (n-s) contacts. T, total contacts; L, lateral contacts perpendicular to the boundary; P, parallel to the boundary. (B‴) Relative total signal intensity (average for n-n contacts set at one), and % of signal concentrated in puncta (green surfaces in B'). Error bars: SD. *$p < 0.05$ and ***$p < 10^{-6}$, Student's t test. Cell interfaces (17 to 32) from seven independent experiments were measured for each category.

(C) Immunolocalization of endogenous C-cadherin. Tilted 3D reconstitution of a 10-μm-thick horizontal section from a whole embryo. Arrows point to cadherin puncta; arrowheads point to the characteristic bright smooth pattern found at the boundary. (C′) Quantification of puncta density and relative total signal intensity for endogenous cadherin. Most puncta observed along the boundary coincided with the edge of lateral homotypic contacts (yellow arrows in C), in which case they were excluded from quantification, the resolution being insufficient to allocate them to one type of contacts. Error bars: SD. *$p < 0.05$, Student's t test, 12 boundaries, six independent experiments.

(D) Colocalization of C-cadherin, β-catenin, and α-catenin. Vertical projection of five z planes. Note that the membranes appear slanted in this projection. (D′) Enlarged image showing a typical concentration of cadherin puncta (yellow arrows) forming a lateral junction at the edge of homotypic contacts. Concave arrowheads point to additional puncta decorating the homophilic contact and flat arrowheads to the smooth cadherin pattern along the boundary. (D″) Line scans (dotted line in D) for Che-α-catenin and C-cadherin-YFP signals. Arrows point at the edges of two lateral junctions that flank the homotypic contact (n-s). The ratio between α-catenin and C-cadherin was similar for smooth membranes and puncta.

(E) YFP-p-120ctn also shows the typical smooth boundary pattern (arrowheads). Arrows: puncta at homotypic contacts. Vertical projection of six z planes.

(F) Expression of membrane-targeted Cherry confirms the tight membrane apposition at the boundary (arrowheads).

See also Figure S1.

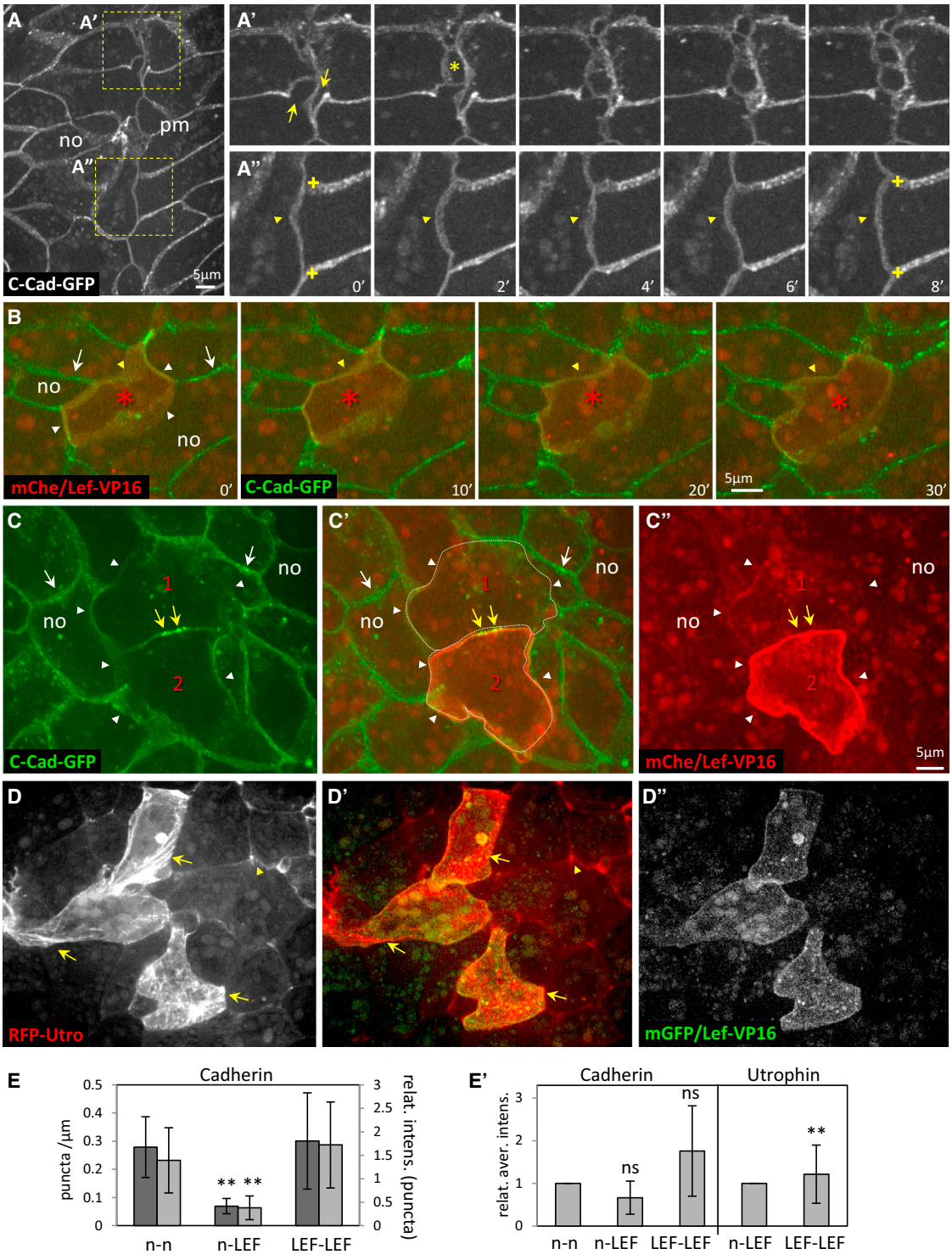

Figure 2. Plasma Membrane Dynamics at the Notochord Boundary

(A–A″) Frames from time-lapse confocal movie of explant expressing C-cadherin-GFP (Movie S1). Vertical projection of four z planes. (A) General view with position of the areas enlarged in (A′) and (A″). (A′) Transient formation and retraction of multiple interdigitations at the boundary. Arrows: connection between cell body and protrusion. Asterisk: section of a digitation. (A″) Typical "flagging" of the boundary membranes (arrowheads). Note the stable position of the lateral membranes (crosses).

(B and C) Cell-autonomous inhibition of cadherin clustering at heterotypic contacts in mosaic embryos. Single presomitic cells were induced in the notochord field by injection of a plasmid coding for constitutively active LEF-VP16 (Reintsch et al., 2005). Cells were traced in live explants through membrane Cherry (red), expressed by the LEF-VP16 plasmid under the control of a separate promoter (see the Experimental Procedures). Each image is a vertical projection of multiple

(legend continued on next page)

found configurations in which two LEF-VP16-expressing cells formed a pair in the notochord (Figure 2C). Whereas heterotypic contacts with the surrounding notochord cells were much smoother than were normal homotypic contacts (Figure 2C, arrowheads), bright cadherin clusters formed specifically at contacts between the LEF-VP16-positive cells (Figure 2C, yellow arrows). These patterns were quantified: heterotypic contacts had slightly decreased total cadherin levels but had four times fewer puncta than did normal homotypic contacts (Figures 2E and 2E'). The fraction of cadherin concentrated in puncta was proportionally decreased too (Figure 2E). Homotypic contacts between two LEF-VP16 cells, on the contrary, gave comparable values to those of notochord homotypic contacts for all three parameters. We conclude that the "boundary-like" smooth cadherin pattern of LEF-VP16 cells in the notochord was not due to a general loss of cell-cell adhesion but resulted specifically from the heterotypic nature of their contacts with notochord cells. Note that some LEF-VP16-expressing cells may have not yet fully developed presomitic properties, which may explain the slightly higher average puncta density of puncta measured at ectopic heterotypic contacts compared to the endogenous boundary.

Consistent with their failure to establish adhesive cadherin contacts with adjacent notochord cells, LEF-VP16-expressing cells showed slug-like movements and seemed to be squished by the notochord cells (Figure S2D), which accounts for their random migration (Reintsch et al., 2005). Their actual sorting from the notochord to the presomitic mesoderm was very difficult to image at high resolution, because of their unpredictability and rapidity (Reintsch et al., 2005). In the very few cases (only three cells) in which we were able to record the early contact with the presomitic tissue, the intensity of the cadherin signal increased instantaneously, indicating the immediate formation of dense clusters (Figure S2E, arrows). Thus, the decision to remain integrated or to sort could be fully explained by the ability or inability to form these puncta according to the identities of the contacting cells.

Evidence for Tensile Structures and for Blebbing-like Behavior at the Boundary

The fact that yolk platelets were completely excluded from the boundary area (Figures 1B and 1D) was indicative of the presence of a particularly thick layer of cortical cytoskeleton, which could be responsible for the peculiar membrane behavior. Indeed, a prominent accumulation of filamentous actin marked the position of the boundary as reproducibly as the smooth cadherin pattern (Figure 3A and quantification in Figure S4). This enrichment was confirmed in fixed, nonmanipulated whole embryos (Figure S3A). Single LEF-VP16-expressing cells in the notochord exhibited massive accumulation of filamentous actin into extensive stress fiber-like structures (Figures 2D and 2E′), consistent with the fact that these cells were completely surrounded by heterotypic contacts.

Live analysis revealed the existence of two types of actin structures, which differed with regard to their relationship with the plasma membrane and could be clearly distinguished during outward bulging of the membrane (Figure 3A; Movie S2): the first one consisted of a continuous layer closely lining the membranes on both sides of the boundary, and following all their undulating and protrusive movements (red arrowheads). The second corresponded to a network of actin fibers (red arrows), which maintained a stationary position, oriented roughly parallel to the boundary (highlighted in diagrams of Figure 3A). The two structures remained connected by sparse links, prominently at both sides of the forming bulges or protrusions (arrowheads). At these anchoring points, the membranes showed steep bends, whose orientation seemed dictated by that of the actin filaments. Numerous membrane invaginations were constantly pulled inside the cell (white concave arrowheads). These images clearly reflected tensile actin-based structures connected intermittently to the plasma membrane. We confirmed the existence of prominent contractile structures along the boundary by detecting accumulation of phosphorylated myosin light chain in fixed samples (Figure S3B). Live imaging of myosin light chain revealed that this structure was made of discontinuous fibers (Figures 3B and 3C), formed by local transient bursts (data not shown).

The actin and myosin pattern and the membrane dynamics were strikingly reminiscent of the classical blebbing behavior observed in some cell types (Charras and Paluch, 2008). The protrusions formed a continuum with blebs that filled the gap of the boundary (Figure 3C′, asterisks) created on the most ventral side of the explants by the removal of the archenteron roof (Figure 1A″, thin dotted red line equivalent to superficial focal planes). The high similarity to classical blebs was further confirmed by high levels of Dia1, but not of Arp3 or of Ena, colocalizing with the membrane-associated pool of actin at the boundary interface and in the protrusions (Figures 3E, 3E′, and S3 and quantifications in Figure S4). Dia1 is thought to participate in the assembly of a new cortex that is responsible for bleb retraction (Charras and Paluch, 2008). Note, however, that Dia1 was also found along homotypic contacts and thus was not a unique feature of the boundary. All forms of blebs and protrusions observed along the boundary showed identical characteristics, indicating

z planes. (B) mCherry/LEF-VP16-positive cell (asterisk) surrounded by wild-type notochord cells. Cadherin largely failed to cluster at heterotypic contacts (white arrowheads), although forming numerous puncta at homotypic notochord contacts (arrows). The yellow arrowhead follows the typical "flagging" behavior of a heterotypic contact. (C) Example of two mCherry/LEF-VP16-positive cells, labeled 1 and 2, showing strong cadherin puncta at homotypic contacts (yellow arrows). White arrowheads and arrows point, respectively, to smooth cadherin signal at heterotypic contacts and to clusters between notochord cells.
(D) Massive accumulation of filamentous actin (Cherry-utrophin mRNA, red) in cells coexpressing membrane GFP/ LEF-VP16 (green). Note stress fiber-like structures spanning through the cell (arrows). Wild-type notochord cells showed low utrophin signal, except at corners joining three cells (arrowhead).
(E and E′) Quantification. (E) Cadherin puncta density at wild-type notochord contacts (n-n), heterotypic contacts between LEF-VP16-expressing and wild-type notochord cells (n-LEF), and homotypic contacts between LEF-VP16-expressing cells (LEF-LEF). Seven individual experiments were quantified. (E′) Average cadherin and utrophin intensities relative to homotypic contacts. Twelve instances from five individual experiments were quantified. Error bars: SD. $^{**}p < 0.01$; ns, not significant.
See also Figure S2.

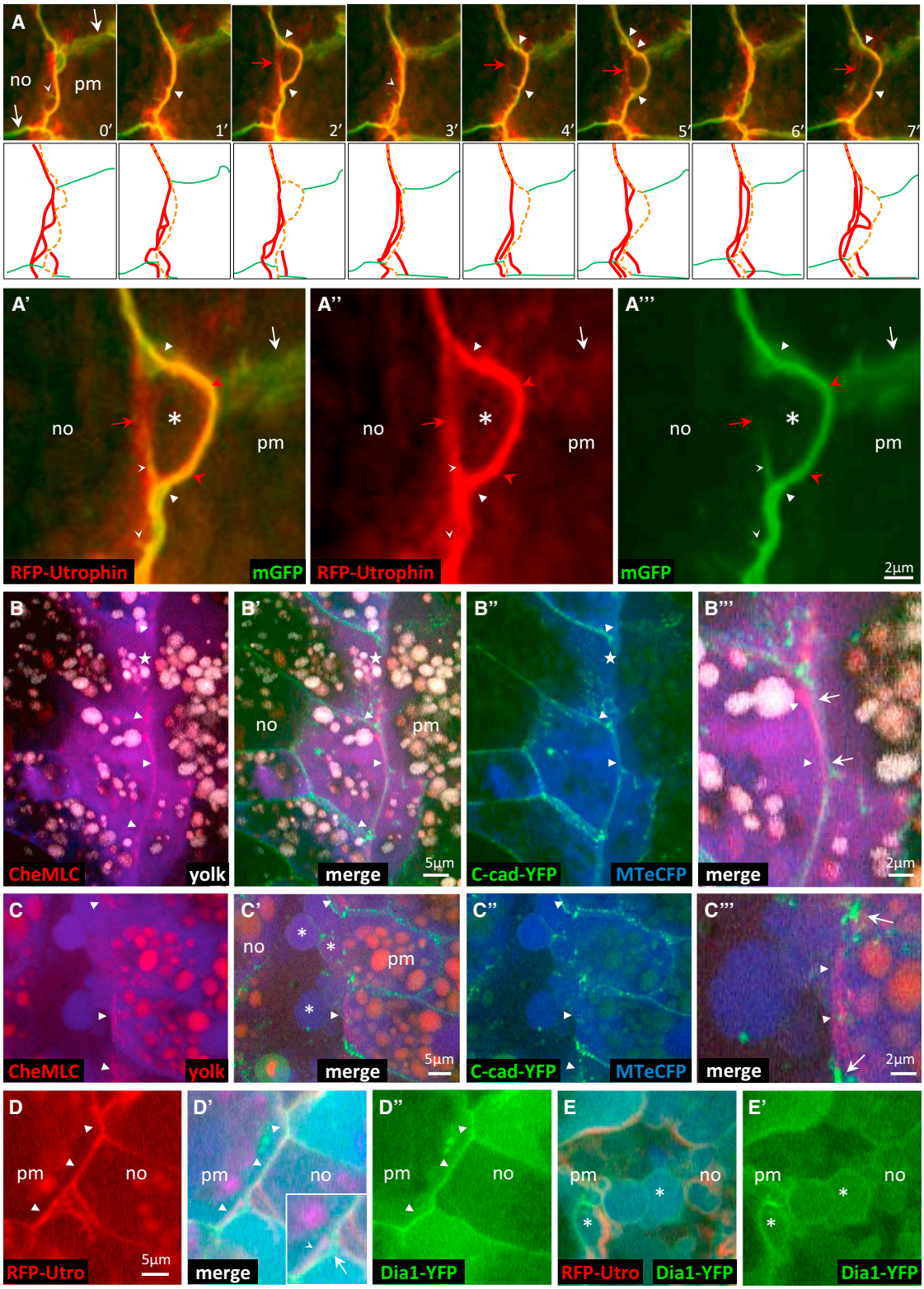

Figure 3. Evidence for Dynamic Contractile Structures and Blebbing-like Membrane Behavior along the Boundary

(A) Live imaging of the plasma membrane (mGFP) and cortical filamentous actin (Red-utrophin). Frames are taken from Movie S2. Vertical projection of six z planes. (A′–A′′′) Enlarged view from frame #2. Red arrowheads point to the membrane-associated pool, and red arrows point to the network of fibers, from which the membrane separated during formation of bleb-like protrusions (asterisks). White arrowheads: Actin anchor points and corresponding membrane bends. Concave white arrowheads: deep transient membrane invaginations pulled along and/or toward the actin network. White arrows: sparse actin along homotypic

(legend continued on next page)

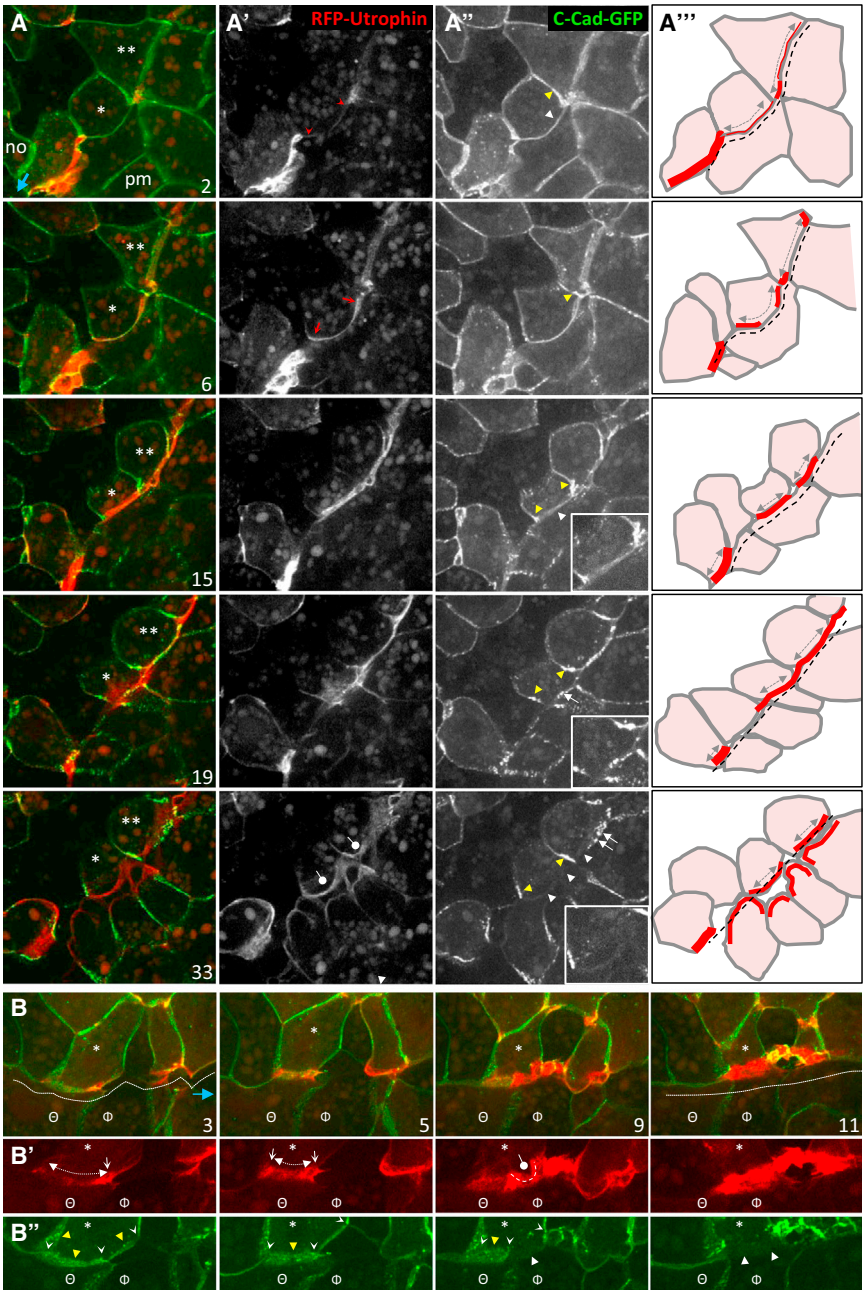

Figure 4. Live Imaging of the Establishment of the Boundary

(A) General view of cells just posterior to the boundary, the end of which is visible at the bottom left (blue arrow). Selected frames from Movie S3; frame time interval = 5 min. Vertical projection of three focal planes. At the start of the sequence, the notochord cell labeled * had just initiated the characteristic development of separation behavior. Its anterior neighbor was already in contact with the mature boundary. Its posterior neighbor, labeled **, had started the process slightly ahead but appeared delayed at the end of the sequence. (A′) Actin. A faint line marked the future boundary interface in frame #2 (cell edges marked by red arrowheads). The signal increased in the following frames, starting from the edges (#6, red arrows). Blebbing appeared in #33 (round head arrows). (A″) Cadherin. Yellow arrowheads: increased accumulation at lateral junctions. #15, white arrowhead: temporary smooth membrane. #19, white arrow: phase of strong, but transient, cadherin clusters. #33, arrowheads: final smooth cadherin pattern for cell *. (A‴) Diagram of cell outlines and actin accumulation (red). Double arrows highlight the contractile oscillations, and the dashed line indicates the straightening of the boundary.

(B–B″) Detail of a cell (*) undergoing transition from homotypic to heterotypic contact. Vertical projection of three planes. The mature boundary is outside of the field (blue arrow in #3). White concave arrowheads: edges of the two future heterotypic contacts between cell * and cells Φ and Θ. #3: The boundary (dotted jagged line) was first marked by actin accumulation, starting at one of the cell edges and then the second edge (white arrows). Cell contacts initially displayed mild cadherin clustering (yellow arrowheads). #5: The interface with cell Θ contracted (dotted double arrows). #9, contact with cell Φ: massive increase in actin, start of blebbing (bullet and curved dashed line), complete loss of puncta, and dramatic decrease in cadherin signal (white arrowhead). #11: Actin accumulation spread through the whole interface and the boundary straightened (dotted line). See also Table 1.

that they corresponded to different morphological manifestations of the same phenomenon. We conclude that the boundary is characterized by contractile structures that exert high tension oriented roughly parallel to the tissue interface and provide the plasma membrane with bleb-like properties. We hypothesized that this phenomenon could be the actual cause of cadherin cluster inhibition and ultimately of tissue separation.

contacts. The drawings below each frame highlight the approximate positions of fluctuating membrane and associated actin (dashed orange line) and of the comparably more stationary network (red lines).

(B and C) Live imaging of explants expressing MLC-Cherry (red), C-cadherin-YFP (green), and eCFP (blue), used as soluble cytoplasmic marker. Vertical projections of four z planes. (B) Deep focal plane. MLC-positive fibers concentrated along the boundary (arrowheads). Note that the signal is inhomogeneous and discontinuous (star). (B‴) Enlarged view: the strongest MLC signal (arrowheads) is separated from the boundary membranes (cadherin signal, arrows). (C) Superficial focal plane. Bleb-like structures (asterisks) protrude beyond the MLC fibers (arrowheads). (C‴) Detail of MLC fibers.

(D and E) Actin-Dia1 colocalization at the boundary (arrowheads). (D) Deep focal plane. Insert: detail of Dia1 membrane accumulation (arrow) and actin fibers connecting the two basal sides of a bulge (concave arrowhead). (E) Superficial focal plane with numerous blebs (asterisks).

See also Figures S3 and S4.

Table 1. Characteristic Events during Formation of the Notochord Boundary

Structures/Molecules Involved	Process	Frequency
actin cytoskeleton	initial thin line marks the future boundary[a]	78%
actin cytoskeleton	early accumulation at lateral edges[a]	90%
C-cadherin	cluster concentration on lateral contacts, formation of homotypic lateral junctions[a]	81%
actin cytoskeleton	progressive accumulation along the boundary interface	100%
cell morphology	cycles of cell contraction (direction parallel to heterotypic contacts)	100%
C-cadherin	cycles of appearance/disappearance of transient strong heterotypic puncta[b]	61%
cell morphology	straightening of the boundary	100%
actin cytoskeleton	blebbing[a,c]	71%
C-cadherin	permanent smooth cadherin pattern at heterotypic contacts[a,c]	71%
C-cadherin	general increase in clustered cadherin at homotypic contacts within tissues[d]	60%

A series of stereotypical changes were observed that were identified by studying the distribution of filamentous actin, clustering of C-cadherin, and cell morphology. Thirty explants were analyzed, and the percentage of instances in which a given event was detected is provided in the rightmost column.

[a]The start or the end of the process was missing from several recordings, accounting for the fact that early and late events scored lower percentages.

[b]This phase was absent at contacts that progressed particularly rapidly toward complete separation.

[c]The final disappearance of transient clusters precisely coincided with the appearance of blebs.

[d]The first and the last frames were compared. Note that the initial degree of clustering was variable.

Early Events during Establishment of the Notochord Boundary

Boundary formation is a continuous process that takes place in the region of the dorsal mesoderm that has just involuted (Figure 1A‴). By imaging the cells immediately posterior to the end of the visible boundary, we were able to follow the changes that preceded the appearance of the mature boundary (Figures 4A and 4B; Movie S3). Compared to the cells in the more anterior region, where notochord and presomitic mesoderm have separated (Figure 4A, frame #33), the cells of the newly involuted mesoderm appeared rounder and exhibited less prominent C-cadherin clustering (Figure 4A, frame #2), probably reflecting the fact that they were not yet under the strong tension exerted by convergence-extension movements. The process leading to boundary formation occurred within a 3- to 5-cell-wide region. It did not appear to be strictly coordinated, because the onset and the duration varied between neighboring cells (Figures 4A and 4B). Each individual cell, however, followed a stereotypical sequence, described in detail in the legend of Figure 4 and summarized in Table 1. The process can be described as follows: the position of the future boundary was first marked by a faint signal for filamentous actin (Figure 4A′, #2; Figure 4B′, #3). Actin then started to massively accumulate, first near the cell edges and then all along the interface (Figure 4A′, frames #6–#19). Cadherin distribution changed relatively early on, with accumulation at lateral junctions (Figure 4A″, yellow arrowheads). Along the heterotypic interface, it sometimes became rapidly smooth but often first went through a phase of strong, but unstable, clustering (Figure 4A″, white arrows). Remarkable oscillations in the length of heterotypic contacts clearly reflected contractions directed parallel to the boundary interface (Figures 4A‴and 4B′, dotted double arrows). The boundary straightened during this phase. The final smooth cadherin pattern of the mature boundary was invariably reached simultaneously with the start of blebbing (Figures 4A″ and 4B″, white arrowheads). Collectively, these observations indicate that increased contractility at heterotypic contacts is an early and quite dramatic event that may control other aspects of boundary formation, including changes in cadherin distribution and ultimately tissue separation.

Myosin Activity Is Required for Cell Sorting and Tissue Separation

To assess the role of contractile structures, we first tested the effect of interfering with myosin activation on cell sorting between the notochord and the presomitic mesoderm. We used our mosaic assay in which a small number of cells of the presumptive dorsal mesoderm are manipulated by plasmid DNA injection, and the percentage of these cells located in the notochord is scored at the end of gastrulation (Reintsch et al., 2005). Control cells (e.g., expressing GFP, Figure 5B) tend to distribute relatively evenly between both tissues, but cells expressing the Lef-VP16 fusion construct are efficiently excluded from the notochord and accumulate in the adjacent presomitic mesoderm (<5% miss-sorting, Figures 5A and 5B). Interference with the Rho pathway by expression of either a dominant-negative RhoA variant or the Rho-binding domain of Rhotekin significantly impaired cell sorting of Lef-VP16-expressing cells (Figures 5A′ and 5B). Sorting was also inhibited by incubation of whole embryos in the presence of the ROK inhibitor Y26732 or the MLCK inhibitor ML7 (Figure 5C). The weaker effect of these soluble inhibitors was expected because of limited diffusion through the large embryo. Note that an effect of myosin inhibition on cell migration could not explain our results, because even in the absence of migration LEF-VP16-expressing cells would have been expected to cluster with other abutting cells of the same presomitic fate, and those clusters should have formed boundaries with notochord cells. On the contrary, all manipulated cells appeared well integrated in the notochord (Figure 5A″, asterisk; Figure S2B). Thus, inhibition of the Rho-ROK and MLCK pathways appeared to affect the actual ability to discriminate between homotypic and heterotypic contacts. We directly tested the role of myosin on the endogenous boundary by treating dorsal mesoderm explants, in which cells had free access to soluble molecules, with the myosin ATPase inhibitor blebbistatin. Blebbistatin caused rapid fusion of the notochord boundary (Figure 5D, arrows; Figure 5E). We then asked if myosin activity was responsible for preventing cadherin clusters

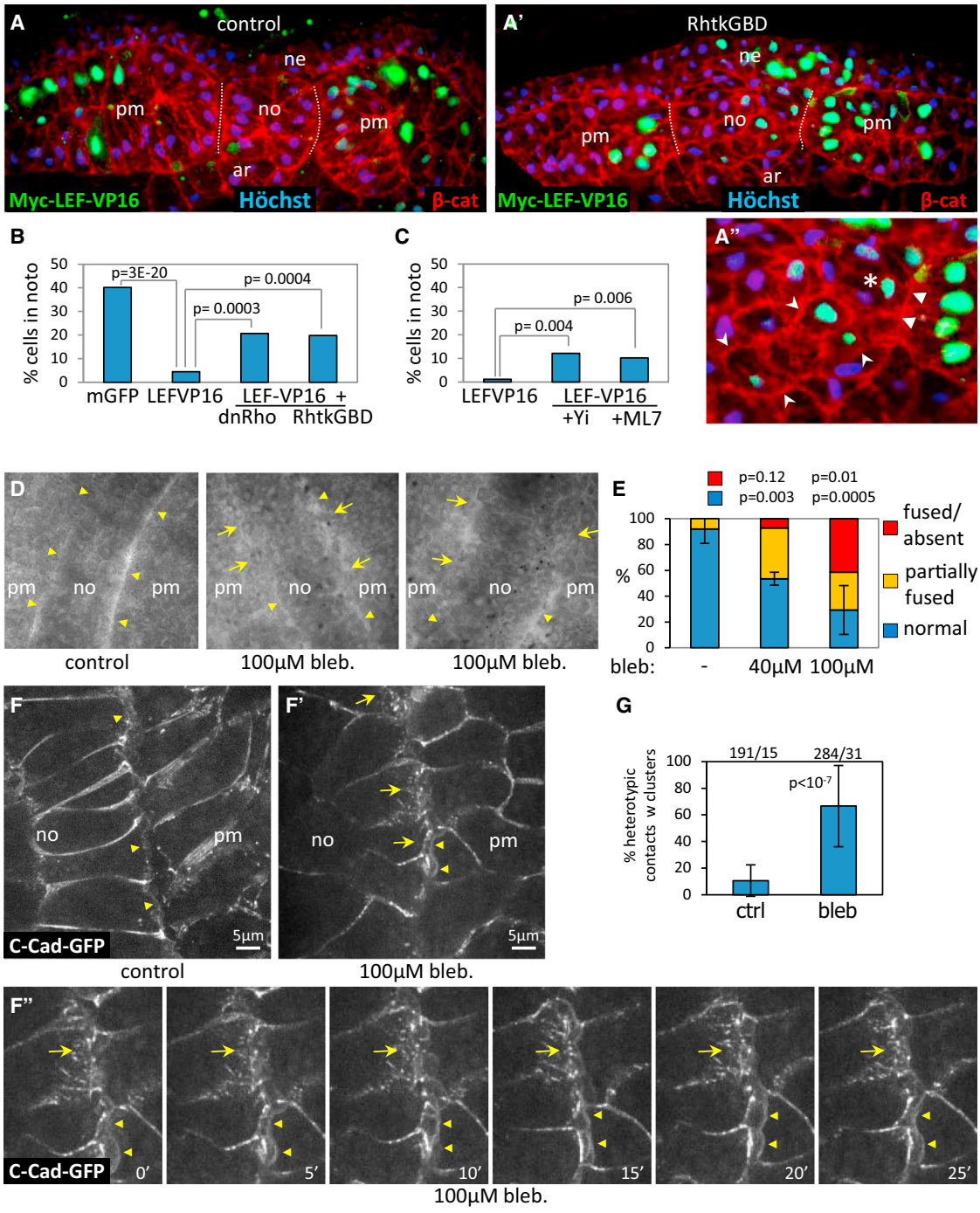

Figure 5. Myosin Activity Is Required for Cell Sorting and Inhibition of Cadherin Clustering

(A–C) Inhibition of Rho/ROK /MLCK interferes with cell sorting in mosaic embryos. (A and A′) Transversal sections showing cells expressing LEF-VP16 (detected through its myc-tag, green) alone or coexpressed with the Rho inhibitor construct GTPase Binding Domain of Rhotekin (RhtkGBD). Plasma membranes were stained for β-catenin, and nuclei were stained with Höchst. Boundaries are indicated with dotted lines. (B and C) Quantification. Control cells distributed evenly between both tissues (~40% in the notochord). LEF-VP16-induced presomitic cells were almost completely excluded from the notochord. Sorting was inhibited by coexpression of dominant negative Rho (dnRho) or RhtkGBD (B) or incubation of the whole embryo in the presence of ROK (Y27632) or MLCK (ML-7) inhibitors (C).

(D and E) Inhibition of myosin II ATPase activity by blebbistatin causes fusion of the notochord boundary in a dose-dependent manner. (D) Examples of bright field images. Arrowheads: regular boundaries; arrows: partially fused boundaries (arrows). (E) Quantification. Boundaries were scored as "normal," "partially fused" (approximately half of the length intact), or "fused or absent" (less than one-fourth intact). Error bars: SD.

(F and G) Blebbistatin treatment induces cadherin clustering and cell mixing across the notochord boundary. Frames from confocal movies of C-cadherin-GFP-expressing dorsal explants. Vertical projection of six focal planes. (F) Control explant. Arrowheads point to the smooth cadherin pattern along the boundary.

(legend continued on next page)

at the boundary. After blebbistatin treatment, we observed massive formation of cadherin clusters at heterotypic contacts along the notochord-presomitic mesoderm interface (Figure 5F′, arrows). These contacts were stable (Figure 5F″, arrow), demonstrating that myosin inhibition was indeed sufficient to reverse inhibition of adhesion between these two tissues. This cellular phenotype was robust and highly reproducible (Figure 5G). We conclude that myosin activity acts upstream of cadherin-mediated adhesion in notochord separation and that it is required for both proper cell sorting and boundary behavior. Note that, consistent with the boundary remnants observed at low magnification (Figure 5D), the areas of intimate cadherin contacts (Figure 5F′, arrows) were interspersed with residual blebs (arrowheads). These blebs tended to be much more static (Figure 5F″; Movie S4), which is the characteristic effect of blebbistatin and is consistent with myosin being required for bleb retraction and restoration of "normal" cortical properties (Charras and Paluch, 2008). Importantly, cadherin clusters still failed to appear at the blebs (Figure 5F″, arrowheads).

Ephrin/Eph Signaling Is Required for Cell Sorting, Myosin Activation, and Cadherin Regulation at the Boundary

We then investigated the source of the signal that triggers myosin activation at heterotypic contacts. We considered ephrins and Eph receptors as the first candidates and screened their expression pattern in notochord and presomitic tissues by qRT-PCR (Figure S5A). We found that EphB4 and ephrinB2, its most effective ligand in the *Xenopus* system (N.R., R. Winklbauer, and F.F., unpublished data), were expressed in complementary patterns, with EphB4 being highly enriched in the presomitic mesoderm and ephrinB2 being more abundant in the notochord (Figures 6A and S5A). Thus, the ephrinB2-EphB4 pair looked like a good candidate to mediate repulsion at heterotypic contacts between the two tissues. We also found a high enrichment of EphA4 in the notochord. Although the selectivity of EphA4 is still not well defined, we also included EphA4 in our functional analysis because it appears to be systematically expressed in asymmetric patterns and functionally involved at other embryonic boundaries (Cooke et al., 2005; Park et al., 2011; Watanabe et al., 2009; N.R., R. Winklbauer, and F.F., unpublished data).

In the mosaic assay, LefVP16-expressing cells completely failed to sort in embryos injected with antisense morpholino oligonucleotides (MO) targeting ephrinB2, EphB4, or EphA4 (Figures 6B′ and 6C). EphrinB2, EphA4, or EphB4 MOs and dominant-negative EphB4 (EphB4ΔC) also severely disrupted the endogenous boundary (Figures 6D and 6E′) without affecting cell fate (Figure 6G′). The effect of EphA4 and B4 MOs was specifically observed when they were targeted to the tissue expressing high levels of the corresponding receptor (Figure 6D).

Interference with ephrin/Eph signaling drastically decreased and often completely erased p-MLC accumulation along the boundary (Figures 6F′ and S5B). p-MLC levels inversely correlated with the levels of MOs (reflected by the coinjected GFP marker) and with the severity of the boundary phenotype. Note that the p-MLC signal at contacts within the tissue was similar in the notochord and the presomitic mesoderm and seemed insensitive to ephrin/Eph interference (Figure S5B). We conclude that increased p-MLC at the notochord boundary is specifically and entirely dependent on ephrin/Eph signaling. The perfect correlation between acute myosin activation and the presence of an organized boundary (e.g., arrowheads in Figure 6F′) further supports our hypothesis that myosin activation downstream of ephrins/Ephs is responsible for notochord separation.

We also examined the effect of ephrin/Eph loss of function on cadherin at the boundary by live confocal microscopy (Figure 6H; Movie S5). EphA4 MO, EphB4 MO, and EphB4ΔC efficiently caused extensive overlap of notochord and presomitic cells. Bleb-like structures were largely, but not completely, absent (Figures 6H and 6H′, flat arrowheads, and Figure 6J) and numerous cadherin clusters appeared at heterotypic contacts (Figures 6H and 6H′, concave arrowheads, and Figure 6I). We conclude that ephrins and Ephs are the contact cues that control separation at the notochord boundary.

DISCUSSION

The Notochord Boundary Is the Product of Local Reactions

Previous models for tissue separation have opposed three major mechanisms, cell-cell adhesion, cortical tension, and contact inhibition. Our findings bring these three parameters into a single coherent description of tissue separation. The key feature of the system resides in the local control at sites of heterotypic contact. The traditional models of differential adhesion or tension, sensus stricto, assumed that the characteristics of the system could be inferred from the global properties of the two tissues and that adhesion and tension at the boundary should represent some middle point between those of each separate population (Harris, 1976; Krieg et al., 2008; Maître et al., 2012; Manning et al., 2010; Steinberg, 1970). Based on our observations, the central role of the balance between tension and adhesion enunciated in the classical biophysical models of cell sorting (Harris, 1976; Steinberg, 1970) still holds true, but these two parameters are now subordinated to spatially restricted signals instructed by ephrins and Ephs (Figure 7A). This repulsion-based mechanism enables cells to switch rapidly and reversibly from full adhesion at homotypic contacts to low or even no adhesion at heterotypic contacts, which explains the efficiency and speed of sorting of notochord and presomitic cells (Reintsch et al., 2005) and the sharpness and straightness of the boundary.

Inhibition of Adhesion Is under the Control of Myosin Contractility

The deficit in cadherin clusters provides a molecular explanation for the low adhesiveness of the tissue boundary interface. This property could not have been predicted based on the characteristics of the two tissues taken in isolation: notochord and

(F′) Blebbistatin-treated explant (see Movie S4). Arrows: cadherin puncta at contacts between notochord and presomitic cells. Arrowheads: blebs with smooth cadherin distribution. (F″) Detail of selected frames from the same movie. Arrows: dense puncta at contacts. Arrowheads: blebs remain much more stable than in controls (compare with Figure 2A and Movies S1, S2, and S3). (G) Quantification. Numbers on top indicate number of scored cells and number of embryo explants (five independent experiments). Error bars: SD.

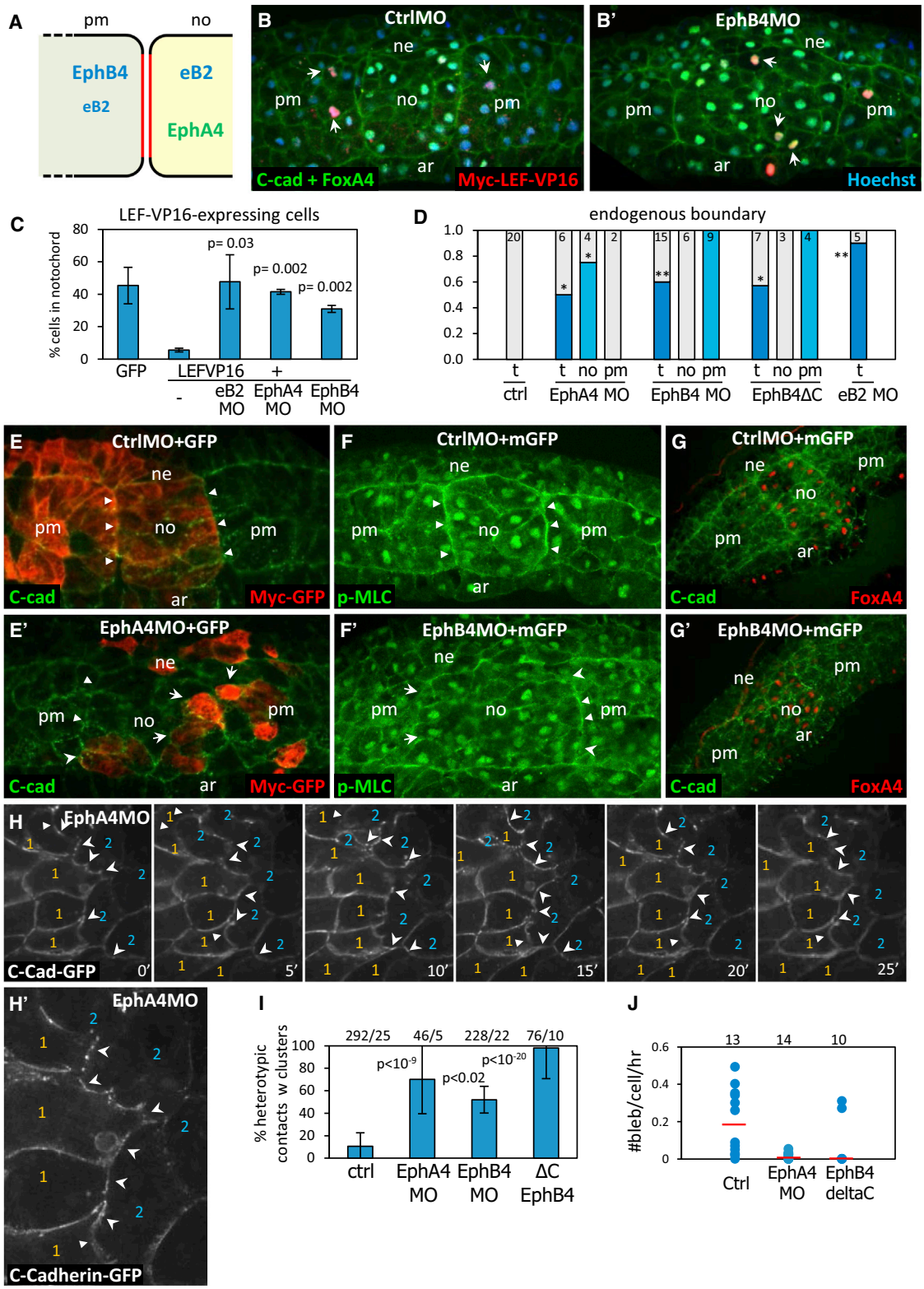

Figure 6. Ephrin/Eph Signaling Is Required for Cell Sorting, Myosin Activation, and Inhibition of Cadherin Clustering at the Notochord Boundary

(A) Scheme of differential expression of ephrinB2, EphA4, and B4 in the dorsal mesoderm (see relative values in Figure S5).

(B and C) Ephrin/Eph depletion blocks sorting of LEF-VP16-expressing cells. LEF-VP16 DNA was coinjected with control (B) or Ephrin/Eph morpholino oligonucleotides (MO) (B′). Sections were stained for myc-tagged LEF-VP16 (red nuclei), C-cadherin (green membranes), FoxA4 (green nuclei), a nuclear marker for

(legend continued on next page)

presomitic mesoderm homotypic contacts are indeed qualitatively and quantitatively undistinguishable (Figures 1A and 1B). The strong propensity to concentrate cadherins in clusters at homotypic contacts and the equally strong resilience for clustering at heterotypic contacts also accounts for the surprising ability of cells to sort properly, independently of cadherin levels (Reintsch et al., 2005).

The massive accumulation of actomyosin fibers and the visible signs of high tension along the boundary were also not predicted by the differential adhesion and differential tension hypotheses. Here, we provide direct demonstration that ephrin signaling-dependent myosin activity is responsible for the inhibition of cadherin clustering and for tissue separation (although we do not exclude the possible contribution of additional mechanisms).

Myosin activity is known to influence cell-cell adhesion, both negatively, by creating cortical tension, and positively, by stimulating a mechanosensing α-catenin-vinculin link to the actin cytoskeleton (Huveneers et al., 2012; Yonemura et al., 2010). In *Xenopus* mesoderm tissues, p-MLC does colocalize with cadherin at homotypic contacts (Figure S3C′), but blebbistatin did not seem to affect these contacts under our experimental conditions, whereas it stimulated formation of new cadherin clusters across the boundary. The high contractility of this interface is presumably incompatible with adhesion. During establishment of boundary, we did observe an intermediate phase at which heterotypic contacts seemed to resist to the waves of contraction by engaging more cadherins into puncta (Figure 7B). This phenomenon is highly reminiscent of the classical tension-dependent reinforcement of integrin focal contacts (Schwartz and DeSimone, 2008; Puklin-Faucher and Sheetz, 2009). After this phase of tug of war, however, cadherin adhesions disappeared concomitant with the appearance of blebs.

Note that the mechanism uncovered here departs from the simplest intuitive model of de-adhesion, where contractility would prevent adhesive bonds by physically pulling the two apposing membranes apart. Here, on the contrary, the membranes were pressed against each other by the outward movement caused by blebbing. The fact that cadherin clustering failed despite this close physical apposition suggested that high tension created an unfavorable membrane-cytoskeleton configuration.

Actomyosin activity is also elevated at *Drosophila* compartment and *Xenopus* ectoderm-mesoderm boundaries (Monier et al., 2010; Landsberg et al., 2009; Aliee et al., 2012; N.R., R. Winklbauer, and F.F., unpublished data). The actomyosin structures observed in *Drosophila* were presented as "supracellular cables" (Monier et al., 2010; Landsberg et al., 2009; Aliee et al., 2012), but this description would be an oversimplification in the case of the notochord boundary. The actin cortical network does span the entire length of the cell contacts, but myosin positive cables are discontinuous and transient and depend on local ephrin signals. Whether similar dynamic systems control other boundaries will be an exciting area of research for future studies.

Similarities and Differences with the Ectoderm-Mesoderm Boundary

We have now added the notochord boundary to the list of vertebrate boundaries that depend on ephrin-Eph signaling. The situation at the notochord boundary is particularly complex, with at least two ephrinBs and five cognate receptors as well as additional ephrinAs and EphAs (Figure S5; data not shown) expressed in the notochord and presomitic mesoderm at different levels. Although we do not yet have a complete picture of the specificity of the various ephrin/Eph pairs, the strength of the loss-of-function phenotypes and their specific impact on local myosin activation constitute compelling evidence for a key role of these molecules.

The degree of adhesion/repulsion at tissue interfaces appears well adjusted to accommodate the specific requirements of each system: the near-complete lack of adhesion at the notochord-presomitic mesoderm boundary seems to be an extreme case. These tissues must be able to slide freely relative to each other for proper convergence-extension (Keller

axial tissues (notochord, floor plate and archenteron roof), and Höchst (blue nuclei). Eph-depletion caused a significant number of LEF-VP16-expressing cells to remain inside the notochord (arrows). (C) Quantification from three independent experiments. p values correspond to comparison with LEF-VP16 alone. Error bars: SD.

(D–F) Interference with ephrin/Eph function perturbs the formation of the endogenous boundary. Embryos were injected with MOs or EphB4ΔC mRNA, together with Myc-GFP mRNA as a tracer. (D) Quantification. Each boundary was given a score of 0 (intact), 0.5 (partially disrupted), or 1 (absent). Columns represent the average score; the number of analyzed boundaries is indicated on top. Three categories of embryos were counted for Eph MO interference: total (t), notochord-targeted (no), or presomitic-targeted (pm) injection. The boundaries were strongly disrupted or absent in all cases in which the injection targeted the tissue expressing high levels of the corresponding Eph (A4 in the presomitic mesoderm, B4 in the notochord). Injections targeted to the opposite tissue had no effect. *$p < 0.02$; **$p < 0.001$, seven independent experiments. (E and E′) Examples of control and disrupted boundaries. Sections were immunostained for C-cadherin (green) and Myc-GFP, used as tracer (red). Flat arrowheads: Normal boundary. Concave arrowheads: Partial disruption of a boundary bordered by Myc-GFP/EphA4 MO-positive notochord cells (concave arrowhead). Arrows: Boundary absent, a group of injected cells spanning the area between notochord and presomitic mesoderm. (F and F′) MLC activation at the boundary requires ephrin/Eph signaling. (F) Strong continuous accumulation of p-MLC staining along the boundaries of control MO-injected embryos (arrowheads). (F′) Partial (concave arrowheads) or complete (arrows) loss of p-MLC signal at the boundary in EphB4 MO-injected embryo. Images for other ephrin/Eph interfering conditions are presented in Figure S5.

(G and G′) Ephrin/Eph depletion does not affect notochord cell fate. FoxA-positive notochord was still clearly identifiable in EphB4 MO-injected embryos, despite severely disrupted boundaries.

(H–J) Interference with ephrin/Eph function causes cadherin clustering across the boundary. (H) Frames from Movie S5, EphA4 MO-injected explant expressing cadherin-GFP. Notochord cells and presomitic cells, marked, respectively, with orange "1" and blue "2" had extensively intercalated. Numerous cadherin puncta were observed at heterotypic contacts (concave arrowheads). Flat arrowheads: remaining blebs. (H′) Detail of frame 20'. (I) Quantification: percentage of cells with clusters at the notochord-presomitic mesoderm interface. Five independent experiments. Error bars: SD. (J) Quantification of blebbing activity. Only unambiguous blebbing was quantified. Membrane undulations ("flapping"), although similarly inhibited by Eph depletion, were not easily measurable. Five independent experiments.

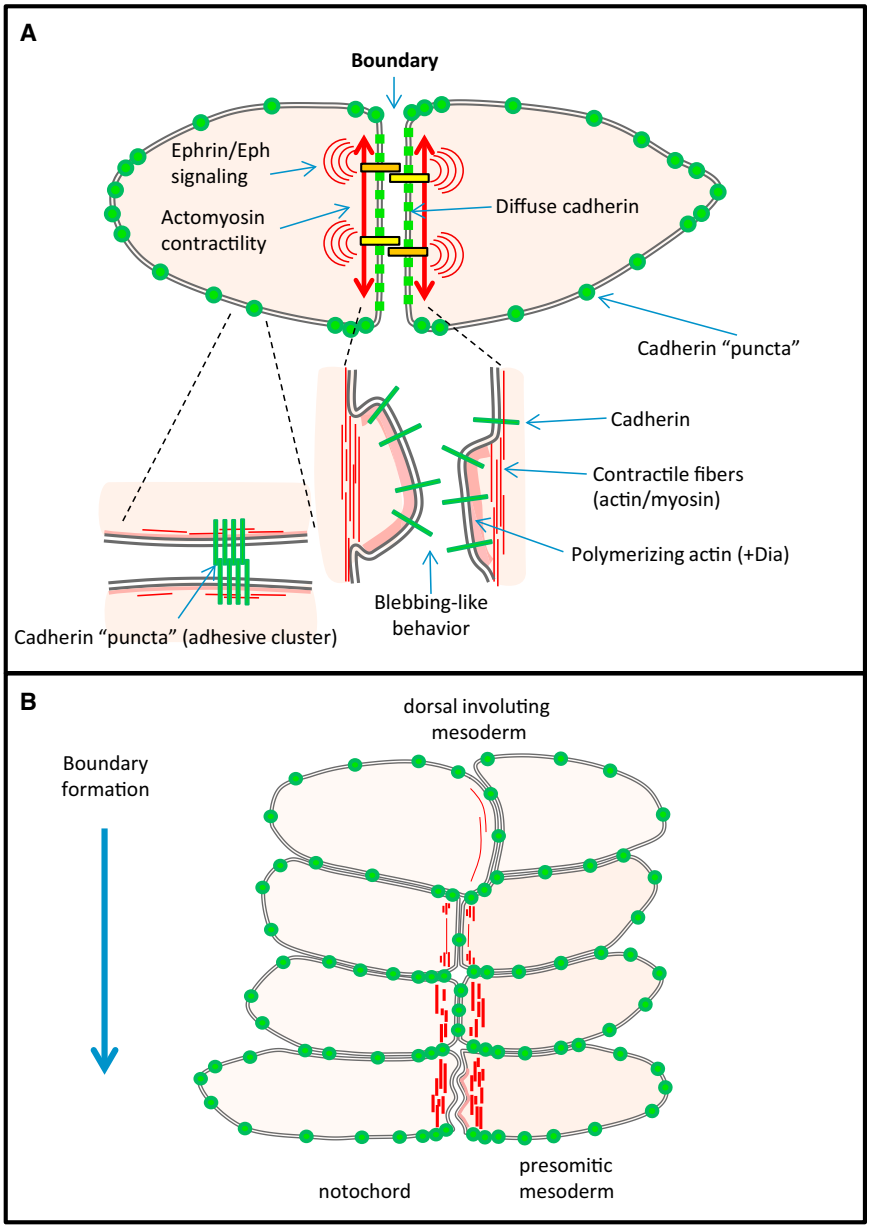

Figure 7. Model of Regulation of Cell-Cell Adhesion at the Boundary

(A) Cell-cell contact-dependent signals generate cortical contraction, which inhibits cadherin clustering. Cadherins are represented in green; the actin cytoskeleton is represented in red; and ephrin/Eph are represented in yellow and orange. Low contractility along the lateral cell contacts is compatible with intimate cell-cell adhesion mediated by cadherin clusters. Ephrin-Eph signaling across the boundary triggers increased local contractility, which causes detachment of the plasma membrane from the actin cortex and prevents cadherin clustering. The resulting interface displays high membrane dynamics and very low cell-cell adhesion (dotted green line). The accumulation of filamentous actin and Dia1 along the membrane of the blebs corresponds to the rapid reformation of a submembranous actin layer involved in bleb retraction.

(B) Summary of the events leading to the emergence of the boundary. Contractile fibers assemble along the future boundary. Progressive actin accumulation is accompanied by strong cortical contraction and by changes in cadherin localization: lateral connections are progressively reinforced, while a transient increase in clustering is observed across the boundary. Eventually, the cortical tension reaches sufficient levels to trigger membrane blebbing (or equivalent membrane undulations; data not shown), and cadherin adhesions are stably inhibited.

See also Movie S3.

et al., 1989). Furthermore, somitic and notochord fates remain highly labile during these stages (Domingo and Keller, 1995), and the system may not tolerate contacts between the two cell types very well. Significant adhesion must be maintained at the ectoderm-mesoderm boundary, because the mesoderm uses the ectoderm surface as a substrate for migration. Blebs are rarely observed (data not shown), and temporary adhesive contacts are frequently established (Rohani et al., 2011), probably corresponding to the intermediate situation observed during formation of the notochord boundary (Figure 7B). We speculate that the same inhibitory action of cortical contraction on cadherin adhesion represents a general mechanism that controls vertebrate tissue separation, which would manifest itself under different forms depending on the intensity of ephrin-Eph signaling and on other factors, such as the basal contractile and adhesive states of the tissues.

EXPERIMENTAL PROCEDURES

Live Imaging of Dorsal Mesoderm Explants

mRNA coding for various fluorescent fusion proteins were injected in the two-cell-stage embryo to obtain widespread expression in the dorsal mesoderm. mRNAs were titrated to achieve low levels of expression that would not interfere with normal development. In some experiments, single cells were labeled/manipulated by injection of plasmid DNA at the 8-cell. Dorsal explants were dissected at the late gastrula stage and imaged using a spinning disc confocal microscope.

Immunofluorescence

Cryosectioning and immunofluorescence were performed as described previously (Schohl and Fagotto, 2002; Fagotto and Brown, 2008).

Image Processing and Quantification

Images were analyzed using ImageJ. Most figures display vertical projection of several z planes. For quantification, cadherin puncta were identified on longitudinal line scans of membranes in single focal planes. The width of the line was set to include the whole thickness of the cadherin signal. A threshold was set based on cadherin average intensity, and peaks above threshold were counted as puncta. Direct visual counting of spots on the original images, both on single planes and on three-dimensional (3D) reconstitutions, confirmed the values obtained. Membrane localization of cytoskeleton components was quantified on broad transversal line scans.

Detailed experimental procedures can be found in the Supplemental Experimental Procedures.

SUPPLEMENTAL INFORMATION

Supplemental Information includes Supplemental Experimental Procedures, five figures, and five movies and can be found with this article online at http://dx.doi.org/10.1016/j.devcel.2013.09.004.

ACKNOWLEDGMENTS

We are thankful to Drs. Bill Bement, André Brändli, Ken Cho, Gergana Gateva, Barry Gumbiner, Rolf Kemler, Pierre McCrea, Elena Pasquale, Naoki Watanabe, and Alpha Yap for their generous gift of plasmids and antibodies. We thank Laura Canty for her critical reading of our manuscript. This work was supported by grants from the Natural Sciences and Engineering Research Council of Canada (261679-03) and Canadian Cancer Society Research Institute (017162/700915) (to F.F.). This work is dedicated to Dr. Ray Keller, a pioneer in the field and mentor to us all.

Received: December 7, 2012
Revised: June 26, 2013
Accepted: September 4, 2013
Published: October 3, 2013

REFERENCES

Adams, C.L., Chen, Y.T., Smith, S.J., and Nelson, W.J. (1998). Mechanisms of epithelial cell-cell adhesion and cell compaction revealed by high-resolution tracking of E-cadherin-green fluorescent protein. J. Cell Biol. *142*, 1105–1119.

Aliee, M., Röper, J.C., Landsberg, K.P., Pentzold, C., Widmann, T.J., Jülicher, F., and Dahmann, C. (2012). Physical mechanisms shaping the *Drosophila* dorsoventral compartment boundary. Curr. Biol. *22*, 967–976.

Cavey, M., Rauzi, M., Lenne, P.F., and Lecuit, T. (2008). A two-tiered mechanism for stabilization and immobilization of E-cadherin. Nature *453*, 751–756.

Charras, G., and Paluch, E. (2008). Blebs lead the way: how to migrate without lamellipodia. Nat. Rev. Mol. Cell Biol. *9*, 730–736.

Chen, X., and Gumbiner, B.M. (2006). Paraxial protocadherin mediates cell sorting and tissue morphogenesis by regulating C-cadherin adhesion activity. J. Cell Biol. *174*, 301–313.

Cooke, J.E., Kemp, H.A., and Moens, C.B. (2005). EphA4 is required for cell adhesion and rhombomere-boundary formation in the zebrafish. Curr. Biol. *15*, 536–542.

Domingo, C., and Keller, R. (1995). Induction of notochord cell intercalation behavior and differentiation by progressive signals in the gastrula of *Xenopus laevis*. Development *121*, 3311–3321.

Durbin, L., Brennan, C., Shiomi, K., Cooke, J., Barrios, A., Shanmugalingam, S., Guthrie, B., Lindberg, R., and Holder, N. (1998). Eph signaling is required for segmentation and differentiation of the somites. Genes Dev. *12*, 3096–3109.

Fagotto, F., and Brown, C.M. (2008). Detection of nuclear β-catenin in *Xenopus* embryos. Methods Mol. Biol. *469*, 363–380.

Foty, R.A., and Steinberg, M.S. (2005). The differential adhesion hypothesis: a direct evaluation. Dev. Biol. *278*, 255–263.

Harris, A.K. (1976). Is Cell sorting caused by differences in the work of intercellular adhesion? A critique of the Steinberg hypothesis. J. Theor. Biol. *61*, 267–285.

Heasman, J., Crawford, A., Goldstone, K., Garner-Hamrick, P., Gumbiner, B., McCrea, P., Kintner, C., Noro, C.Y., and Wylie, C. (1994a). Overexpression of cadherins and underexpression of β-catenin inhibit dorsal mesoderm induction in early *Xenopus* embryos. Cell *79*, 791–803.

Heasman, J., Ginsberg, D., Geiger, B., Goldstone, K., Pratt, T., Yoshida-Noro, C., and Wylie, C. (1994b). A functional test for maternally inherited cadherin in *Xenopus* shows its importance in cell adhesion at the blastula stage. Development *120*, 49–57.

Huveneers, S., Oldenburg, J., Spanjaard, E., van der Krogt, G., Grigoriev, I., Akhmanova, A., Rehmann, H., and de Rooij, J. (2012). Vinculin associates with endothelial VE-cadherin junctions to control force-dependent remodeling. J. Cell Biol. *196*, 641–652.

Keller, R., Cooper, M.S., Danilchik, M., Tibbetts, P., and Wilson, P.A. (1989). Cell intercalation during notochord development in *Xenopus laevis*. J. Exp. Zool. *251*, 134–154.

Kemp, H.A., Cooke, J.E., and Moens, C.B. (2009). EphA4 and EfnB2a maintain rhombomere coherence by independently regulating intercalation of progenitor cells in the zebrafish neural keel. Dev. Biol. *327*, 313–326.

Krieg, M., Arboleda-Estudillo, Y., Puech, P.H., Käfer, J., Graner, F., Müller, D.J., and Heisenberg, C.P. (2008). Tensile forces govern germ-layer organization in zebrafish. Nat. Cell Biol. *10*, 429–436.

Landsberg, K.P., Farhadifar, R., Ranft, J., Umetsu, D., Widmann, T.J., Bittig, T., Said, A., Jülicher, F., and Dahmann, C. (2009). Increased cell bond tension governs cell sorting at the *Drosophila* anteroposterior compartment boundary. Curr. Biol. *19*, 1950–1955.

Lee, C.H., and Gumbiner, B.M. (1995). Disruption of gastrulation movements in *Xenopus* by a dominant-negative mutant for C-cadherin. Dev. Biol. *171*, 363–373.

Maghzal, N., Vogt, E., Reintsch, W., Fraser, J.S., and Fagotto, F. (2010). The tumor-associated EpCAM regulates morphogenetic movements through intracellular signaling. J. Cell Biol. *191*, 645–659.

Maître, J.L., Berthoumieux, H., Krens, S.F., Salbreux, G., Jülicher, F., Paluch, E., and Heisenberg, C.P. (2012). Adhesion functions in cell sorting by mechanically coupling the cortices of adhering cells. Science *338*, 253–256.

Manning, M.L., Foty, R.A., Steinberg, M.S., and Schoetz, E.M. (2010). Coaction of intercellular adhesion and cortical tension specifies tissue surface tension. Proc. Natl. Acad. Sci. USA *107*, 12517–12522.

Medina, A., Swain, R.K., Kuerner, K.M., and Steinbeisser, H. (2004). *Xenopus* paraxial protocadherin has signaling functions and is involved in tissue separation. EMBO J. *23*, 3249–3258.

Monier, B., Pelissier-Monier, A., Brand, A.H., and Sanson, B. (2010). An actomyosin-based barrier inhibits cell mixing at compartmental boundaries in *Drosophila* embryos. Nat. Cell Biol. *12*, 60–65.

Moore, S.W., Keller, R.E., and Koehl, M.A. (1995). The dorsal involuting marginal zone stiffens anisotropically during its convergent extension in the gastrula of *Xenopus laevis*. Development *121*, 3131–3140.

Park, E.C., Cho, G.S., Kim, G.H., Choi, S.C., and Han, J.K. (2011). The involvement of Eph-Ephrin signaling in tissue separation and convergence during Xenopus gastrulation movements. Dev. Biol. *350*, 441–450.

Puklin-Faucher, E., and Sheetz, M.P. (2009). The mechanical integrin cycle. J. Cell Sci. *122*, 179–186.

Ratheesh, A., and Yap, A.S. (2012). A bigger picture: classical cadherins and the dynamic actin cytoskeleton. Nat. Rev. Mol. Cell Biol. *13*, 673–679.

Reintsch, W.E., Habring-Mueller, A., Wang, R.W., Schohl, A., and Fagotto, F. (2005). beta-Catenin controls cell sorting at the notochord-somite boundary independently of cadherin-mediated adhesion. J. Cell Biol. *170*, 675–686.

Rohani, N., Canty, L., Luu, O., Fagotto, F., and Winklbauer, R. (2011). EphrinB/EphB signaling controls embryonic germ layer separation by contact-induced cell detachment. PLoS Biol. *9*, e1000597.

Schohl, A., and Fagotto, F. (2002). β-catenin, MAPK and Smad signaling during early *Xenopus* development. Development *129*, 37–52.

Schwartz, M.A., and DeSimone, D.W. (2008). Cell adhesion receptors in mechanotransduction. Curr. Op. Cell Biol. *20*, 551–556.

Steinberg, M.S. (1970). Does differential adhesion govern self-assembly processes in histogenesis? Equilibrium configurations and the emergence of a hierarchy among populations of embryonic cells. J. Exp. Zool. *173*, 395–433.

Steinberg, M.S., and McNutt, P.M. (1999). Cadherins and their connections: adhesion junctions have broader functions. Curr. Opin. Cell Biol. *11*, 554–560.

Takeichi, M. (1995). Morphogenetic roles of classic cadherins. Curr. Opin. Cell Biol. *7*, 619–627.

Tepass, U. (1999). Genetic analysis of cadherin function in animal morphogenesis. Curr. Opin. Cell Biol. *11*, 540–548.

Tepass, U., and Hartenstein, V. (1994). The development of cellular junctions in the *Drosophila* embryo. Dev. Biol. *161*, 563–596.

Vasioukhin, V., Bauer, C., Yin, M., and Fuchs, E. (2000). Directed actin polymerization is the driving force for epithelial cell-cell adhesion. Cell *100*, 209–219.

Wacker, S., Grimm, K., Joos, T., and Winklbauer, R. (2000). Development and control of tissue separation at gastrulation in *Xenopus*. Dev. Biol. *224*, 428–439.

Watanabe, T., Sato, Y., Saito, D., Tadokoro, R., and Takahashi, Y. (2009). EphrinB2 coordinates the formation of a morphological boundary and cell epithelialization during somite segmentation. Proc. Natl. Acad. Sci. USA *106*, 7467–7472.

Winklbauer, R. (2009). Cell adhesion in amphibian gastrulation. Int. Rev. Cell Mol. Biol. *278*, 215–275.

Yonemura, S., Wada, Y., Watanabe, T., Nagafuchi, A., and Shibata, M. (2010). alpha-Catenin as a tension transducer that induces adherens junction development. Nat. Cell Biol. *12*, 533–542.